



HAL
open science

Suitable interface for coupling liquid chromatography to inductively coupled plasma-mass spectrometry for the analysis of organic matrices. 1 Theoretical and experimental considerations on solute dispersion

Marie Bernardin, Frédérique Bessueille-Barbier, Agnès Le Masle,
Charles-Philippe Lienemann, Sabine Heinisch

► To cite this version:

Marie Bernardin, Frédérique Bessueille-Barbier, Agnès Le Masle, Charles-Philippe Lienemann, Sabine Heinisch. Suitable interface for coupling liquid chromatography to inductively coupled plasma-mass spectrometry for the analysis of organic matrices. 1 Theoretical and experimental considerations on solute dispersion. *Journal of Chromatography A*, 2018, 1565, pp.68-80. 10.1016/j.chroma.2018.06.024 . hal-01858414

HAL Id: hal-01858414

<https://hal.science/hal-01858414>

Submitted on 8 Nov 2018

HAL is a multi-disciplinary open access archive for the deposit and dissemination of scientific research documents, whether they are published or not. The documents may come from teaching and research institutions in France or abroad, or from public or private research centers.

L'archive ouverte pluridisciplinaire **HAL**, est destinée au dépôt et à la diffusion de documents scientifiques de niveau recherche, publiés ou non, émanant des établissements d'enseignement et de recherche français ou étrangers, des laboratoires publics ou privés.

1 **Suitable interface for coupling Liquid Chromatography to Inductively Coupled**
2 **Plasma-Mass Spectrometry for the analysis of organic matrices. 1 theoretical**
3 **and experimental considerations on solute dispersion**

4 *Marie Bernardin^{1,2}, Frédérique Bessueille-Barbier¹, Agnès Le Masle², Charles-Philippe*
5 *Lienemann², Sabine Heinisch*¹*

6 *(1) Université de Lyon, Institut des Sciences Analytiques, UMR 5280, CNRS, ENS Lyon, 5 rue de*
7 *la Doua, 69100 Villeurbanne, France*

8 *(2) IFP Energies nouvelles, Rond-point de l'échangeur de Solaize, BP 3, 69360 Solaize France*

9 * Corresponding author : Tel : +33 437 423 551 ;

10 E-mail address : sabine.heinisch@univ-lyon1.fr (Sabine Heinisch)

11 **Abstract**

12 Liquid chromatography (LC) hyphenated to a specific detection such as inductively coupled
13 plasma-mass spectrometry (ICP-MS) is a technique of choice for elemental speciation
14 analysis. However, various instrumental limitations may considerably reduce the expected
15 sensitivity of the technique. Among those, we were interested by the solute dispersion into
16 the interface located between LC and ICP-MS. The interface consists of a Sample
17 Introduction System (SIS) and a possible flow-splitter prior to SIS. Flow splitting can be
18 required in case of organic matrices to reduce the organic solvent amount entering plasma
19 which may lead to plasma instabilities.

20 Although extra-column dispersion is usually well taken into account with conventional
21 UV detection it has been little studied in the context of LC-ICP-MS and moreover never
22 quantified. Our objective is to assess the loss in column plates and hence in both separation
23 quality and sensitivity which may be generated by the coupling of LC and ICP-MS in the
24 specific case of organic matrices. In this first study, this is done (1) from a theoretical
25 approach; (2) from 55 experimental studies reported in LC-ICP-MS and (3) from our
26 experimental results highlighting the critical impact of the flow splitter on extra-column
27 dispersion depending on both flow-rate and split ratio. It turns out by evaluating the 55
28 reported studies by means of theoretical calculations, that the loss in plates due to extra-

29 column dispersion was most of the time beyond 50 % and even often beyond 90 %.
30 Moreover, from our experiments, it has been shown that a very low split ratio (1:50) could
31 generate an additional variance around $200 \mu\text{L}^2$ which induces a loss in theoretical plate of
32 90 % for ultra-high performance LC (UHPLC) column (5 cm x 2.1 mm, 1.7 μm).

33 **Keywords**

34 Speciation - Liquid chromatography - Inductively coupled plasma - Extra-column dispersion -
35 Sample introduction system - LC-ICP-MS – Flow splitting

36 **1. Introduction**

37 The need for determining elemental species concentrations rather than total element
38 concentrations has grown within the past decades. According to Templeton et al. [1,2]
39 speciation analysis consists in identifying and quantifying different chemical species of a
40 particular element in a given sample. It has become an important field of research over the
41 past few years in several areas including biochemistry, environmental chemistry,
42 ecotoxicology, pharmaceuticals, petrochemicals, and nutrition science [3].

43 Nowadays hyphenated techniques such as Liquid Chromatography (LC) hyphenated with
44 Inductively Coupled Plasma Mass Spectrometry (LC-ICP-MS) are widely used both to obtain
45 elemental information and to discriminate species in a given matrix. LC techniques, including
46 ion exchange chromatography (IEC) [4], reversed-phase liquid chromatography (RPLC) [5],
47 ion-pairing chromatography (IPC) [6], size exclusion chromatography (SEC) [7,8] and
48 hydrophilic interaction liquid chromatography (HILIC) [9,10], have been used for speciation
49 analysis [11]. Different hyphenated techniques can be combined together to achieve more
50 exhaustive characterization of complex matrices. For example, LC-ESI-MS can be associated
51 to LC-ICP-MS to obtain both structural information and elemental information [5,12–14].

52 Most speciation analyses are performed in aqueous matrices by using ion-exchange
53 chromatography and deal with environmental samples [15]. In this specific case, the mobile
54 phase is not critical for the coupling of both techniques since the amount of organic solvent
55 in the mobile phase is limited (small percentage of organic modifier sometimes added,
56 usually without disturbing plasma stability). However, when using RPLC [16–28] or HILIC
57 [9,10,29–34], a large amount of organic solvent is introduced into the plasma. The problems

58 involved by this introduction was thoroughly discussed by Leclercq et al [35,36] in a recent
59 review.

60 Some key issues have to be considered for coupling LC to ICP-MS in case of organic matrices
61 [3]: (i) metal contamination from the chromatographic system and/or the stationary phase
62 and/or the mobile phase [3], (ii) plasma instabilities due to the solvent load, especially in
63 case of organic mobile phases [3], (iii) signal fluctuations in gradient elution depending on
64 plasma parameters [37] and (iv) solute dispersion into the interface located between LC and
65 ICP-MS. The interface is made of a sample introduction system (SIS) and a possible flow
66 splitter prior to SIS which may be required, in case of organic matrices, to reduce the
67 amount of solvent entering plasma and hence to decrease plasma instabilities [3]. The solute
68 dispersion in the interface unit is a critical issue because that can result in additional solute
69 band broadening and hence in significant loss in both sensitivity and separation quality.
70 Although extra-column dispersion is usually well taken into account with conventional UV
71 detection, it has been little studied in the context of LC-ICP-MS. In the present study, we
72 made therefore an attempt to assess the extent to which the interface contributes to solute
73 band broadening. This was done by (i) estimating from published studies the likely loss in
74 plates due to solute dispersion in the interface and (ii) showing the critical impact of the flow
75 splitter on extra-column dispersion depending on both flow-rate and split ratio. To support
76 the first approach, a synoptic table has been built (Table 2) which summarizes 55 studies
77 carried out on organic matrices in LC-ICP-MS and gives, for each study, an estimation of the
78 interface contribution to solute band broadening. A further second part of our study will be
79 dedicated to the comparison of a large number of commercially available SIS regarding the
80 extra-column dispersion.

81 **2. Theoretical considerations**

82 Solute dispersion can be assessed by the peak variance. The total solute dispersion (total
83 variance, σ_{total}^2) comes from both dispersion inside the column (column variance, σ_{col}^2) and
84 extra-column dispersion (extra-column variance, σ_{ext}^2).

85 Extra-column dispersion results from the injection process ($\sigma_{injection}^2$), the different tubing
86 (σ_{tubing}^2) and the detection ($\sigma_{detector}^2$) [38].

87 Because variances can be added if the corresponding dispersion process are independent of
88 each other, the total peak variance can be written as

$$89 \quad \sigma_{total}^2 = \sigma_{col}^2 + \sigma_{ext}^2 \quad (1)$$

90 Similarly, the extra-column variance is the sum of individual contributions according to

$$91 \quad \sigma_{ext}^2 = \sigma_{injection}^2 + \sigma_{tubing}^2 + \sigma_{detector}^2 \quad (2)$$

92 For Gaussian peaks, the total peak variance in volume units can be given by the measured
93 peak width at half peak height ($w_{0.5}$) according to

$$94 \quad \sigma_{total}^2 = \frac{F^2 w_{0.5}^2}{5.54} \quad (3)$$

95 Where F is the mobile phase flow-rate.

96 For very bad peak shapes, the second order central moment has to be used to provide a
97 reliable variance value. These latter, in volume units, is given by

$$98 \quad \sigma_{total,v}^2 = F^2 \frac{\int_0^{\infty} (t - t_R)^2 I(t) dt}{\int_0^{\infty} I(t) dt} \quad (4)$$

99 Where t_R is the mean residence time and $I(t)$ the intensity as a function of time.

100 Extra-column variance can be approximated by removing the column and replacing it by a
101 zero dead volume union connector. In this case, extra-column variance is calculated from
102 Eq. (3).

103 The column variance, expressed in length unit is related to both the column length and the
104 column plate height, H_{col} , by

$$105 \quad \sigma_{col}^2 = L H_{col} \quad (5)$$

106 H_{col} varies with the mobile phase linear velocity, u , and its variation may be fitted by the
107 van Deemter equation [39] or by the Knox equation [40] using reduced parameters h_{col}
108 (H_{col}/d_p) and v ($u \cdot d_p / D_m$, d_p being the average particle diameter and D_m , the molecular
109 diffusion coefficient of the solute in the mobile phase). At the minimum of the curve, typical
110 values for h_{col} and v are 3 and 5 respectively.

111 Considering the solute linear velocity at the time the solute is eluted from the column
112 ($u/(1+k_e)$), k_e being the retention factor at elution), the column variance can be expressed in
113 volume units according to

$$114 \sigma_{col}^2 = \frac{V_0^2(1+k_e)^2 H_{col}}{L} \quad (6)$$

115 V_0 is the column dead volume, related to the column length, the internal diameter, d_i and
116 the column porosity, ε_t by

$$117 V_0 = \pi L \varepsilon_t (d_i^2/4) \quad (7)$$

118 Under isocratic conditions, k_e depends on the retention volume and is given by

$$119 k_e = \frac{V_R}{V_0} - 1 \quad (8)$$

120 Under gradient conditions, k_e depends on both the gradient conditions and the solute
121 properties. However a rough estimation of k_e can be made when the linear solvent strength
122 theory (LSST) can be applied and the solvent strength parameter, S is known [41,42], using
123 the following relation

$$124 k_e = \frac{1}{2.3 S t_0 \frac{\Delta C}{t_G}} \quad (9)$$

125 With t_0 the column dead time, ΔC the gradient composition range, and t_G the gradient time.
126 Typical values of S (S being the absolute value of the slope of of the linear relationship
127 between the logarithm of the retention factor and the stronger solvent volume fraction) are
128 4 for small molecules, 20 for peptides and much higher for larger molecules [42].

129 Thus, From Eqs. (6) and (7), the column variance for a given peak in a given chromatogram
130 can be estimated provided that the column geometry is known, and the retention factor can
131 be determined.

132 Similarly to Eq. (6), the total variance can be written

$$133 \sigma_{total}^2 = \frac{V_0^2(1+k_e)^2 H_{total}}{L} \quad (10)$$

134 Where H_{total} is the total plate height resulting from the two dispersion processes.

135 The ratio, β^2 , between column and total variances corresponds to the ratio between the two
136 plate heights and hence to the ratio between effective and column plate numbers according
137 to

$$138 \quad \beta^2 = \frac{\sigma_{col}^2}{\sigma_{total}^2} = \frac{H_{col}}{H_{total}} = \frac{N_{effective}}{N_{col}} \quad (11)$$

139 Where $N_{effective}$ and N_{col} are effective and column plate numbers respectively.

140 The term, β^2 represents the fraction of remaining plates for a given solute, in given
141 chromatographic and instrumental conditions.

142 The peak height and the resolution between two peaks are inversely proportional to the
143 peak standard deviation (σ). As a result, the fractions of remaining peak height and
144 remaining resolution are given by β .

145 The mobile phase flow-rate is related to the reduced linear velocity by

$$146 \quad F = v \frac{V_0 D_m}{L d_p} \quad (12)$$

147 From Eqs. (6) and (12), Table 1 gives an overview of optimum flow-rates and corresponding
148 column variances ($k_e=3$) depending on both column internal diameter and particle size.

149 Depending on SIS, the flow entering the plasma source is expected to be a critical parameter
150 regarding the performance of ICP-MS. According to Table 1, the internal diameter has to be
151 chosen in accordance with the required flow-rate. However as shown in Fig.1, any decrease
152 in column internal diameter leads to a severe decrease in column variance, and hence to a
153 huge decrease in both plate number and sensitivity if the dispersion in SIS is significant. The
154 percentage of remaining plates was calculated from Eq. (11) as a function of extra-column
155 variance for different column internal diameters and two different particle sizes (5 and
156 1.7 μm). The calculations were performed for a k_e value of 3 and a column length providing
157 10000 plates (Fig.1a. 15 cm with 5 μm and 5 cm with 1.7 μm) and 30000 plates (Fig.1b 15 cm
158 with 1.7 μm). Extra-column variance was considered in the range 0.1 to 1000 μL^2 that covers
159 current LC-UV instruments except nanoLC instruments. With the aim of maintaining more
160 than 80 % of the plates ($\beta^2 > 0.8$) and hence more than 90 % of the peak height ($\beta > 0.9$), it
161 appears that the maximum allowable values for the extra-column variance are (1) 1000 and
162 100 μL^2 for conventional columns (4.6 mm i.d) packed with 5 μm and 1.7 μm particles

163 respectively; (2) 50 and 5 μL^2 for narrow bore columns (2.1 mm i.d) packed with 5 μm and
164 1.7 μm particles respectively; 3 and 0.3 μL^2 for micro bore columns (1 mm i.d) packed with
165 5 μm and 1.7 μm particles respectively. These values are slightly higher for 30000 plates with
166 1.7 μm particles (Fig.1b). With capillary columns (300 μm i.d.), the extra-column variance
167 should be much lower than 0.1 μL^2 . This figure also highlights the range of extra-column
168 variance covered by commercially available HPLC and UHPLC instruments with UV detection.
169 With the objective of reaching 10000 plates, it appears that HPLC-UV instruments are not
170 suitable for conventional columns packed with 1.7 μm particles and that most UHPLC-UV
171 instruments cannot be used with narrow bore columns packed with 1.7 μm particles.
172 Furthermore, even very efficient UHPLC-UV instrument (i.e. extra-column variance as low as
173 5 μL^2) are not suitable for micro bore columns.

174 In this context, it is of prime importance to assess the additional extra-column variance
175 brought by the interface between LC and ICP-MS. Considering the curve shapes in Fig.1, it
176 appears that, in any case, the remaining plates might decrease from 80 % to 70 %, 50 %, and
177 30 % by increasing the extra-column variance by a factor of 2, 5 and 10 respectively.

178 As previously discussed, the interest for LC-ICP-MS in case of organic matrices has
179 significantly grown during the past few years. In our opinion, instrument performances are
180 often not considered enough, methods being developed without prior evaluation of the
181 interface contribution to solute dispersion. To assess the additional dispersion brought by
182 the interface in LC-ICP-MS, 55 studies reported in the area of organic matrix speciation have
183 been reviewed and discussed in term of extra-column dispersion in the next section. With a
184 view to reducing the flow entering SIS, an alternative to the reduction of internal diameter
185 may be the use of a flow-splitter prior to SIS. A T-union was indeed used for quantification
186 with online isotopic dilution [25,43–48]. However such unit may lead to significant additional
187 extra-column band broadening. The contribution of flow splitting to extra-column dispersion
188 is therefore studied in the last section.

189 **3. LC-ICP-MS Interface**

190 Peak band broadening is rarely taken into consideration even when the sample matrix
191 becomes complex. Most of the time, authors work with only a few standards instead of a
192 complex mixture to optimize the separation techniques and even less often on a real

193 sample. For instance, Raber et al. [49] focused on eleven arsenic species using an LC
194 separation prior to ICP-MS detection but, as can be seen, the peaks were poorly resolved. A
195 low measured plate number with respect to the theoretical column plate number, can be
196 due to (i) solute dispersion in the chromatographic system (injection system, tubing, UV-
197 detection), (ii) a loss in column plates (depending on the history of the column), or (iii) an
198 additional dispersion generated by the interface between LC and ICP-MS. The interface
199 consists in a Sample Introduction System (SIS) and a possible flow-splitter prior to SIS which
200 can be required, in case of organic matrices, to reduce the amount of solvent entering
201 plasma and hence to decrease plasma instabilities. SIS is usually divided into two devices, the
202 nebulizer, and the spray chamber. The nebulizer converts the liquid from the separation
203 technique into a heterogeneous aerosol made of different droplet sizes. The aerosol is then
204 usually sorted out in a spray chamber. Larger droplets are carried to the waste while smaller
205 ones are sent to the plasma source for atomization/excitation/ionization [35]. Nebulizers,
206 spray chambers, and flow-splitters represent critical devices for ensuring a high-performance
207 coupling. Particular attention must be paid both to the quality of the aerosol produced
208 through the nebulizer/spray chamber [50] and to the contribution of the whole interface to
209 peak band broadening [3,44,45,51–53], both features being able to significantly affect the
210 sensitivity. A well-documented summary of SIS devices was reported by Leclercq and al. [36].
211 Major advantages and drawbacks were discussed in terms of sensitivity and ease of use, but
212 other analytical performances such as efficiency, resolution, sensitivity or extra-column
213 solute dispersion, were not taken into account to compare the different devices. In the
214 present work, this feature has been subjected to a broad exploratory study on 55 published
215 studies (from 1995 to 2017) dealing with the speciation of organic matrices. The
216 corresponding analytical conditions, including LC conditions, type of nebulizers, type of spray
217 chambers and use or not of a flow-splitter, are listed in Table 2 and Table S1 of
218 Supplementary Information, depending on whether enough data were available or not.
219 When data were available (Table 2), an evaluation of the total solute dispersion (total
220 variance, σ_{total}^2) was made from Eq. (3) by considering the most retained peak (symmetrical
221 peaks only). The column variance, σ_{col}^2 , was evaluated from Eq. (6). The extra-column
222 variance, σ_{ext}^2 , was estimated from Eq. (1). To easily compare the percentage of remaining
223 plates (β^2), this value was systematically determined for a retention factor of 3, by column

224 variance rescaling using Eq. (6). Corresponding β^2 values are given in Table 2. The reasons for
225 low β^2 values can be strongly related to the instrument characteristics including the type of
226 interface but also the level of matching between the column geometry and the LC
227 instrument.

228 Fig.2 illustrates the relative distribution of nebulizers and spray chambers used for speciation
229 in LC-ICP-MS in case of organic solvent matrices regarding the dimension of the column
230 used. In many studies, it was difficult to draw relevant conclusions because of a lack of
231 information about SIS and/or the column particle diameter and/or even sometimes, the
232 mobile phase flow-rate. However when the calculations were possible, the following
233 comments can be provided depending on whether the column was conventional, narrow-
234 bore, micro-bore or capillary:

235 *(i) conventional columns:*

236 According to Fig.2, three different nebulizers have been used: pneumatic micro-concentric
237 nebulizer (50 %) operated with flow-rates in the range 40 to 1000 $\mu\text{L}/\text{min}$, pneumatic
238 concentric nebulizer (10 %) operated with flow-rates higher than 1000 $\mu\text{L}/\text{min}$ and hydraulic
239 high-pressure nebulizer (10 %). With the first and second ones [17,20,22,24,25], the liquid is
240 introduced through a horizontal capillary and the gas conducted through an external tube
241 around the liquid capillary. With the third one [54], the liquid is forced through a highly
242 turbulent hydraulic nozzle. Similarly, three different spray chambers are used in association
243 with the preceding nebulizers: cyclonic spray chambers (30 %), double pass spray chamber
244 (20 %) and desolvation units (10 %). With cyclonic spray chambers, the aerosol is tangentially
245 introduced and first impacts against the front walls generate thinner aerosol which is
246 transported towards the injector [50]. The double pass spray chambers is composed of two
247 concentric tubes, the external one promoting droplet elimination through impacts against
248 the wall and reducing aerosol fluctuation due to pump pulsing, the internal one eliminating
249 coarse droplets and inducing a laminar flow aerosol [50]. Finally, desolvation units are
250 designed to reduce the solvent amount into the plasma with either a desolvation membrane
251 to remove organic/hydro-organic matrices in association with a micro-concentric nebulizer
252 [16,54,55] or an ultrasonic nebulizer [56]. The main drawback of desolvation systems is the
253 possible loss of analytes through the desolvation membrane. As reported, the sensitivity

254 achieved with a desolvation micro-concentric nebulizer was dependent on the analyte
255 structure [55,57].

256 When calculations were possible, the calculated percentage of remaining plates (β^2) was
257 found to be lower than 35 % (i.e. 24 [17], 16 % [24], 31 % [20], 14 % [25], 34 % [58]) except in
258 one case (i.e. 86 % [26]). Unfortunately, in this latter case, the information about the
259 interface was not available and as a result, no relevant conclusion could be drawn. As seen in
260 Fig.2 and mentioned earlier, in many cases, the necessary information about nebulizer
261 (30 %) and spray chamber (40 %) was not provided. It is important to note that, with
262 conventional columns leading to high column variance values, the measured loss in plates is
263 likely due either to the interface or to column ageing or to both, but probably not to the
264 contribution of LC instrument to extra-column solute dispersion. As a result, it can be
265 concluded that, in most cases, the separation achieved in the column was partially or
266 completely lost in the interface. As examples, with a micro-concentric nebulizer in
267 association with a Peltier Cooled Cyclonic spray chamber PC³ (supplied by Elemental
268 Scientific), only 24 % of the plates remained [17] and 14 % in association with a double pass
269 spray chamber [25]. It can be noticed that only one study deals with the use of low cyclonic
270 spray chamber among the 55 publications reported [52]. Finally, in association with a
271 desolvation unit, the very bad peak shapes did not allow to conclude about the impact of the
272 interface [54].

273 *(ii) Narrow bore columns*

274 The distribution of the nebulizers was different from that for conventional columns with four
275 different ones used: micro-concentric nebulizers (67 %), parallel path nebulizers (12 %) with
276 the liquid interacting with the high-velocity gas stream coming tangentially into contact with
277 it [50], cross-flow nebulizers (4 %) with liquid and gas outlets perpendicularly mounted on a
278 polymer body and concentric nebulizers (4 %). Most of the time, micro-concentric nebulizers
279 [9,19,21,23,27–29,33,34,47,52,54,59–64] were associated to a cyclonic spray chamber (54 %
280 of the spray chambers used). A specific micro-concentric nebulizer (i.e. microflow PFA-ST or
281 PFA-LC nebulizer supplied by Elemental scientific) was used in several studies [59,61,64]. It is
282 made of a copolymer, with an internal capillary more recessed than other micro-concentric
283 nebulizers [50]. However, very low percentages of remaining plates were estimated in these
284 cases. The highest value was 70 % [52] while all other ones were below 20 % and even some

285 of them below 5 % [29,60]. In the particular study of Vidler et al. [59], the calculated
286 retention factor was found to be lower than 1 (i.e. about 0.5) leading to 16 % of remaining
287 plates only. In this study a micro concentric nebulizer was used, unfortunately, the spray
288 chamber was not mentioned. However, considering a retention factor of 3, the calculated
289 fraction of remaining plates is tremendously improved (i.e. 59 %), suggesting that, in this
290 particular case, the loss in plates was likely due to LC system volumes rather to the interface.
291 Interestingly, the use of two different detectors, ICP-MS and ESI-TOF [33] allowed us to
292 indirectly assess the extra-column dispersion induced by the interface between LC and ICP-
293 MS, assuming no dispersion in both ESI-TOF and ICP-MS. From our calculations, the total
294 variance was 1360 μL^2 with LC-ICP-MS against 490 μL^2 with LC-ESI-MS, thereby leading to an
295 impressive peak variance of 870 μL^2 for the interface alone, far too high considering the
296 expecting narrow-bore column variance (i.e. <200 μL^2 as shown in Table 1). Unfortunately,
297 no information about the interface was available [33] which could have permitted to draw
298 some interesting trends.

299 *(ii) Micro bore and capillary columns*

300 When the column internal diameter is further decreased, the trend is towards the use of
301 total consumption nebulizers (35 % and 18 % for microbore and capillary columns
302 respectively) at the expense of micro-concentric ones (67 %, 47 % and 18 % for narrow-bore,
303 microbore and capillary columns respectively) (Fig.2). Total consumption nebulizers do not
304 require spray chambers or desolvation systems and can work with low flow-rates (typically a
305 few tens of $\mu\text{L}/\text{min}$). The primary aerosol is entirely sent to the plasma. Two different total
306 consumption nebulizers were used with organic/hydro-organic matrices, namely Direct
307 Injection Nebulizer (DIN, supplied by CETAC Technologies) and Direct Injection High-
308 Efficiency Nebulizer (DIHEN, supplied by Meinhard). DIN has been used since 1992 [65] and
309 was often adapted before use [16, 65]. Despite its low volume, highly recommended for
310 hyphenated techniques, its main drawback is its small internal capillary (i.e. 60 μm) which
311 can be easily clogged [36,50]. Moreover, finding the correct distance between the tip and
312 the plasma is not easy considering the capillary thinness. For the above reasons, this
313 nebulizer is no more commercialized [66]. DIHEN is a pneumatic nebulizer in glass or quartz,
314 working with liquid flow-rates between 1 and 100 $\mu\text{L}/\text{min}$. It is characterized by a larger dead
315 volume than DIN. It is therefore always used with an inserted capillary to reduce its dead

316 volume [36,44,45,51,67–69]. The optimum flow-rate for total consumption nebulizers is a
317 few $\mu\text{L}/\text{min}$, which is also the range of flow-rates adapted to capillary LC (i.e. $< 10 \mu\text{L}/\text{min}$ as
318 seen in Table 1). Nevertheless in all studied cases (see Table 2), the estimated percentage of
319 remaining plates was lower than 5 %.

320 Finally, two different SIS (a total consumption nebulizer and a micro-concentric nebulizer
321 combined with a cyclonic spray chamber) were compared for a given capillary column while
322 keeping the same separation conditions [67]. In both cases, the estimated percentage of
323 remaining plates was found to be lower than 1 %, highlighting once again the importance of
324 extra-column band broadening, especially in case of thin columns and the necessity of trying
325 to ensure the lowest possible contribution of the interface.

326 In summary, it has been pointed out that it is essential that the interface is optimized in
327 relation to the separation conditions and especially to the column geometry. In most cases
328 among 26 published chromatograms, the estimated percentage of remaining plates
329 (calculated with a retention factor of 3) were found to be lower than 50 %, 20 %, 5 % and
330 1 % for conventional, narrow-bore, micro-bore and capillary columns respectively. These low
331 percentage values clearly show that the interfacial are mostly inappropriate. Moreover, it is
332 important to point out that the extra column dispersion is never considered. Further
333 investigations were carried out in our Lab to compare commercially available SIS with
334 respect to extra-column dispersion. These results will be extensively discussed in Part II.

335 Adapting the flow-rate before entering SIS can be a good option when using a total
336 consumption nebulizer designed to work at low flow-rates to limit the amount of organic
337 solvent entering the plasma. A zero-dead volume T-union along with suitable tubing can be
338 used to adjust the flow-rate just prior entering SIS [12,25,44,45,67]. Nonetheless, such
339 device is also expected to give rise to additional extra-column dispersion. Zoorob et al. [45]
340 indeed showed that a split ratio of 1:20 generated more dispersion in the interface than DIN
341 alone. However, most authors, using a flow splitter did not consider the additional
342 dispersion generate by such devices [24,25,44,67]. However, it was evaluated under fast
343 separation conditions by injecting, without column, 20 μL of a potassium iodide solution
344 [47]. Flow splitting was used to reduce the acetonitrile concentration and hence to improve
345 ICP-MS performance. The authors visually compared peak shapes with and without flow
346 splitting and deduced that the T-connection did not have a significant impact on the

347 dispersion. However, the comparison was qualitative and not quantitative. To the best of our
348 knowledge, no quantitative study on additional variance brought by flow splitting depending
349 on both flow-rate and split ratio has been reported. This issue is addressed in the next
350 section.

351 4. Determination of peak variance resulting from flow splitting

352 The aim of the present study was to quantify the additional peak variance due to the
353 presence of a flow-splitter. As discussed above, total consumption spray chambers can be
354 used with low flow-rates (up to a few tens of $\mu\text{L}/\text{min}$) to reduce the solvent load into the
355 plasma. However, such flow-rates are much too low when using narrow bore columns (i.e.
356 2.1 mm i.d.) and sub $2\ \mu\text{m}$ particles as usually done in UHPLC. A flow-splitter can be used to
357 solve this problem. It consists in a zero-dead volume T-union located between the column
358 outlet and the detector and intended to divide the main flow into two different flows, the
359 highest being directed to the waste and the lowest to the detector, thereby significantly
360 reducing the flow entering the plasma source. The difficulty may stem from the volumes
361 involved by additional tubing and from the split itself as both may lead to significant
362 additional band broadening, especially when a low split ratio has to be considered. This issue
363 is addressed below by assessing the extra-column variance induced by such device
364 depending on flow-rate, internal diameter of tubing and split ratio.

365 4.1. Material and reagents

366 Methanol was HPLC grade from Sigma Aldrich (Steinheim, Germany). Water was
367 obtained from Elga water purification system (Veolia water STI, Le Pless Robinson, France).
368 Methylparaben was used as test compound and supplied by Sigma-Aldrich (Steinheim,
369 Germany).

370 4.2. Apparatus

371 The instrument used was an Acquity UPLC I-Class 2DLC liquid chromatography system. It
372 includes two high-pressure binary solvent manager with a maximum delivery of $2\ \text{mL}/\text{min}$,
373 an autosampler with a $5\ \mu\text{L}$ injection sample loop, a column oven with a maximum
374 temperature of 90°C and two different detectors (TUV and PDA) with identical flow-cells,

375 leading to identical signal intensity. They can be used one after the other with or without
 376 flow-splitter between both. The wavelength was set at 254 nm with a sampling rate of 40 Hz.
 377 The instrument control was performed by Mass Lynx software. The maximum backpressure
 378 allowed in the first detector cell was 1000 psi.

379 4.3. Procedure and methods

380 The mobile phase was a mixture of 50/50 Water/MeOH (v/v). Methylparaben was
 381 diluted in the same mixture with a concentration of 75 ppm. This study was carried out
 382 without column. All peak variances were calculated from the second order moment of the
 383 peak, Eq. (4), using in-house calculation tool. The injected volume was 1 μ L. A P-727 (0.57 μ L)
 384 T-union was used for flow splitting (from Upchurch, Cluzeau, Sainte-Foy-La-Grande, France).
 385 This T-union was chosen according to a previous study on different commercially available T-
 386 unions which concluded that this one was the best adapted to low dispersion [70]. The set-
 387 up used to measure the peak variance due to flow splitting is shown in Fig.3. Tube #1 was
 388 located between UV-detector #1 and the T-union, Tube #2, between the T-union and UV
 389 Detector #2 (replacing ICP-MS detection for this study) and Tube #3 between the T-union
 390 and the waste. Four different settings were considered. The corresponding tubing
 391 geometries are given in Table 3. The theoretical split ratio, z_{th} , is calculated from the
 392 Poiseuille law, considering the dimensions of Tube #2 and #3, Eq. (13):

$$393 \quad z_{th} = \frac{R_3}{R_3 + R_2} \text{ with } R_i = \frac{L_i}{d_i^4} \quad (13)$$

394 L_i and d_i being the length and the internal diameter of Tube # i respectively.

395 The measured split ratio, z_{meas} , was obtained from the measured flow-rate, F_2 , in Tube #2
 396 ($z_{meas} = F_2/F_1$). In the absence of flow splitting (Setting #A), the split ratio was 1. The difference
 397 between calculated and measured values in Table 3 may be imputed to internal diameter
 398 irregularity.

399 The peak variance due to flow splitting (σ_{split}^2) was assessed by subtracting the sum of the
 400 peak variance measured with Detector #1 (σ_{D1}^2) and that due to Tube #1 ($\sigma_{tubing\ 1}^2$) from the
 401 peak variance measured with Detector #2 (σ_{D2}^2), Eq. (14).

$$402 \quad \sigma_{split}^2 = \sigma_{D2}^2 - \sigma_{D1}^2 - \sigma_{Tub\ #1}^2 \quad (14)$$

403 $\sigma^2_{\text{tubing } 1}$ was measured in the absence of flow splitting with Detector #1 and 2 in series
404 ($\sigma^2_{\text{Tube \#1}} = \sigma^2_{D2} - \sigma^2_{D1}$). It should be noted that σ^2_{D2} corresponds to the total extra-column
405 variance (σ^2_{ext} in Eq. (2)).

406 4.4. Results and discussion

407 Throughout this study, five different settings were studied (Table 3), which differentiated
408 themselves from their measured split ratio and/or their tubing geometry. For the five
409 settings, the dimensions of Tube #1 were the same and hence the variation of $\sigma^2_{\text{Tube \#1}}$ with
410 the total flow-rate (F_1). F_1 was varied in the range 50-700 $\mu\text{L}/\text{min}$, 20-150 $\mu\text{L}/\text{min}$, 50-
411 100 $\mu\text{L}/\text{min}$ and 100-400 $\mu\text{L}/\text{min}$ with settings B, C, D and E respectively. The experimental
412 variation of $\sigma^2_{\text{Tube \#1}}$ with F_1 is given in Fig.4. It could be fitted with an exponential function. As
413 highlighted in Fig.4, the variance increases linearly with the flow-rate up to a value of nearly
414 200 $\mu\text{L}/\text{min}$ and is almost unchanged beyond (i.e. around 8 μL^2). This is in good agreement
415 with reported studies, showing that peak variance values deviate from linearity at high flow-
416 rates with non ideal tubing (i.e. short, coiled and/or rugged tubing) [73].

417 Similarly, the variation of σ^2_{split} with F_1 and hence with F_2 was studied in the presence of the
418 T-union (Fig.5). Two different situations were considered to assess to what extent the peak
419 variance may vary: a decrease in the internal diameter of Tube #2 while keeping the split
420 ratio nearly constant (Setting B and C (Fig.5a)) and a strong decrease in the split ratio while
421 keeping the internal diameter of Tube #2 constant (Setting C, D and E (Fig.5b)).

422 The impact of the internal diameter of Tube #2 was investigated with two different internal
423 diameters, 65 μm (setting B) and 25 μm (setting C). As shown in Fig.5a, the curves,
424 representing the variation of the peak variance with F_2 , are very similar in both cases with
425 only 2 μL^2 difference between both curves, indicating that the internal diameter of Tube #2
426 has little or no impact on the dispersion generated by the split. On the other hand, the
427 impact of the split ratio was found to be very significant as highlighted in Fig.5b. Considering
428 the same resulting F_2 value (e.g. 8 $\mu\text{L}/\text{min}$), the measured peak variance increased from 6 to
429 34 μL^2 with a split ratio decreasing by a factor of about 2 (1:4.8 to 1:9.4), and up to 200 μL^2
430 with a split ratio decreasing by a factor of 10. The impact of the flow splitter on the
431 dispersion can also be visually assessed by comparing the peaks obtained with the different
432 settings. The x-axis is expressed in volume units to have a better comparison of peak

433 broadening. For a given mobile phase flow-rate of 0.1 mL/min, Fig. 6a shows the degradation
434 of the peak shape when the split ratio decreased from 1:1 (no flow splitting) to 1:50 (only
435 2 $\mu\text{L}/\text{min}$ sent to UV-Detector 2). In this latter case, the variance due to the split reached
436 $77\mu\text{L}^2$. When considering a low F_2 value of 10 $\mu\text{L}/\text{min}$ (Fig.6b), the degradation is even more
437 important with $208\mu\text{L}^2$ obtained when the split ratio is decreased down to 1:50. In addition
438 to peak broadening, Fig. 6 clearly points out the problem of sensitivity that can be
439 encountered if the interface and in particular the split device are not carefully chosen.

440 According to Fig.1a, a total extra-column variance of only $100\mu\text{L}^2$ is sufficient to lose more
441 than 70 % of the column plates in UHPLC conditions. Consequently, these results clearly
442 underline the importance of finding the best trade-off between the split ratio which must be
443 high enough, the flow entering ICP-MS which must be low enough and the column flow-rate
444 which must be adapted to UHPLC conditions (typically in the range 400 to 1000 $\mu\text{L}/\text{min}$). In
445 any case, the additional extra-column dispersion brought by flow splitting should be carefully
446 evaluated. Micro-concentric nebulizers can be considered as a good option for the coupling
447 of UHPLC with ICP-MS since they avoid the need for low split ratios. Such nebulizers usually
448 work with flow-rates of around hundreds $\mu\text{L}/\text{min}$ as those required with narrow bore
449 columns. On the other hand, the use of a flow splitter in association with a total
450 consumption spray chamber operated at around 10 $\mu\text{L}/\text{min}$, seems inappropriate for UHPLC
451 purposes.

452 **5. Conclusion and future trends**

453 Within the last number of decades, analytical techniques have evolved from the simple
454 determination of the total amount of a metal element to the determination of its chemical
455 species. In speciation studies, ICP-MS is now routinely coupled with liquid chromatography
456 (LC-ICP-MS).

457 Most applications are performed in an aqueous solvent and are therefore much easier to
458 implement than those needing the introduction of a large amount of organic solvent into the
459 plasma source. Unfortunately, very few analysts pay enough attention to the
460 chromatographic aspects when coupling LC and ICP-MS. During method development,
461 special attention should be focused on extra-column dispersion to minimize it, avoiding
462 excessive dead volume. In view of this article, it clearly appears that efforts need to be made

463 in this specific area before analyzing complex matrix. Indeed, the benefit of method
464 development performed to enhance the analytical performance (resolution and sensitivity)
465 could be lost if solute dispersion in the interface, located between separation and detection
466 devices, is not minimized. A special attention must be paid to a better description of Sample
467 Introduction System since it seems to be the critical part of the coupling and its
468 characteristics are not always specified by the authors. For speciation analysis, it is highly
469 recommended to thoroughly characterize the interface by evaluating extra column
470 dispersion induced by SIS and ensuring that less than 20 % plates are loss. This will be
471 extensively discussed in Part II.

472 Flow splitting can be used with total consumption spray chambers to reduce the flow-rate
473 prior to the sample introduction system but it must be sized properly. As shown in this study,
474 a low split ratio can significantly increase solute dispersion and hence solute dilution. Micro-
475 concentric nebulizers are expected to be more appropriate with possible flow-rates of
476 around hundreds $\mu\text{L}/\text{min}$, thus without the need of flow splitting. Such nebulizers will be
477 compared in the second part of this study which will be devoted to the comparison of
478 commercially available Sample Introduction Systems in term of extra-column dispersion.

479 A last interesting point, in our view, is the impact of extra-column peak broadening on the
480 whole analytical performance when using more complex hyphenated techniques such as 2D-
481 LC-ICP-MS. In the future, if online comprehensive two-dimensional separations are more
482 extensively developed, a particular attention should be paid to the set-up so that every
483 additional dead volume could be assessed in terms of additional dispersion.

484 **References**

- 485 [1] D. m. Templeton, F. Ariese, R. Cornelis, L. g. Danielsson, H. Muntau, H.P. van Leeuwen,
486 R. Lobínski, Guidelines for terms related to chemical speciations and fractionation of
487 elements : definitions, structural aspects, and methodological approaches (IUPAC
488 Recommendations 2000), (2000).
- 489 [2] B. Michalke, Element speciation definitions, analytical methodology, and some
490 examples, *Ecotoxicol. Environ. Saf.* 56 (2003) 122–139. doi:10.1016/S0147-
491 6513(03)00056-3.
- 492 [3] M. Grotti, A. Terol, J. I. Todolí, Speciation analysis by small-bore HPLC coupled to ICP-
493 MS, *Trends Anal. Chem.* 61 (2014) 92–106. doi:10.1016/j.trac.2014.06.009.

- 494 [4] A.A. Ammann, Arsenic speciation by gradient anion exchange narrow bore ion
495 chromatography and high resolution inductively coupled plasma mass spectrometry
496 detection, *J. Chromatogr. A.* 1217 (2010) 2111–2116.
497 doi:10.1016/j.chroma.2010.01.086.
- 498 [5] K.O. Amayo, A. Petursdottir, C. Newcombe, H. Gunnlaugsdottir, A. Raab, E.M. Krupp, J.
499 Feldmann, Identification and Quantification of Arsenolipids Using Reversed-Phase HPLC
500 Coupled Simultaneously to High-Resolution ICPMS and High-Resolution Electrospray
501 MS without Species-Specific Standards, *Anal. Chem.* 83 (2011) 3589–3595.
502 doi:10.1021/ac2005873.
- 503 [6] R. Lohmayer, G.M.S. Reithmaier, E. Bura-Nakić, B. Planer-Friedrich, Ion-pair
504 chromatography coupled to inductively coupled plasma-mass spectrometry (IPC-ICP-
505 MS) as a method for thiomolybdate speciation in natural waters, *Anal. Chem.* 87 (2015)
506 3388–3395. doi:10.1021/ac5046406.
- 507 [7] S.F. Boulyga, V. Loreti, J. Bettmer, K.G. Heumann, Application of SEC-ICP-MS for
508 comparative analyses of metal-containing species in cancerous and healthy human
509 thyroid samples, *Anal. Bioanal. Chem.* 380 (2004) 198–203. doi:10.1007/s00216-004-
510 2699-6.
- 511 [8] V. Vargas, J. Castillo, R. Ocampo Torres, B. Bouyssiére, C.-P. Lienemann, Development
512 of a chromatographic methodology for the separation and quantification of V, Ni and S
513 compounds in petroleum products, *Fuel Process. Technol.* 162 (2017) 37–44.
514 doi:10.1016/j.fuproc.2017.03.027.
- 515 [9] Y. Nygren, P. Hemström, C. Åstot, P. Naredi, E. Björn, Hydrophilic interaction liquid
516 chromatography (HILIC) coupled to inductively coupled plasma mass spectrometry
517 (ICPMS) utilizing a mobile phase with a low-volatile organic modifier for the
518 determination of cisplatin, and its monohydrolyzed metabolite, *J. Anal. At. Spectrom.*
519 23 (2008) 948–954. doi:10.1039/B716093C.
- 520 [10] D. Xie, J. Mattusch, R. Wennrich, Retention of arsenic species on zwitterionic stationary
521 phase in hydrophilic interaction chromatography, *J. Sep. Sci.* 33 (2010) 817–825.
522 doi:10.1002/jssc.200900738.
- 523 [11] J. Delafiori, G. Ring, A. Furey, Clinical applications of HPLC–ICP-MS element speciation:
524 A review, *Talanta.* 153 (2016) 306–331. doi:10.1016/j.talanta.2016.02.035.

- 525 [12] L. Beuvier, Développement d'une méthode de séparation chromatographique couplée
526 aux spectrométries de masse à source d'ionisation électrospray (ESI-MS) et à source
527 plasma à couplage inductif (ICP-MS) : application à l'analyse de spéciation des
528 lanthanides, phdthesis, Université Pierre et Marie Curie - Paris VI, 2015.
529 <https://tel.archives-ouvertes.fr/tel-01381095/document> (accessed October 20, 2016).
- 530 [13] É.R. Pereira, J.F. Kopp, A. Raab, E.M. Krupp, J. del C. Menoyo, E. Carasek, B. Welz, J.
531 Feldmann, Arsenic containing medium and long chain fatty acids in marine fish oil
532 identified as degradation products using reversed-phase HPLC-ICP-MS/ESI-MS, *J Anal*
533 *Spectrom.* 31 (2016) 1836–1845. doi:10.1039/C6JA00162A.
- 534 [14] B. Frindt, J. Mattusch, T. Reemtsma, A.G. Griesbeck, A. Rehorek, Multidimensional
535 monitoring of anaerobic/aerobic azo dye based wastewater treatments by hyphenated
536 UPLC-ICP-MS/ESI-Q-TOF-MS techniques, *Environ. Sci. Pollut. Res. Int.* (2016).
537 doi:10.1007/s11356-016-7075-5.
- 538 [15] K.L. Sutton, J.A. Caruso, Liquid chromatography–inductively coupled plasma mass
539 spectrometry, *J. Chromatogr. A.* 856 (1999) 243–258. doi:10.1016/S0021-
540 9673(99)00580-4.
- 541 [16] L. Bendahl, B. Gammelgaard, Sample introduction systems for reversed phase LC-ICP-
542 MS of selenium using large amounts of methanol—comparison of systems based on
543 membrane desolvation, a spray chamber and direct injection, *J. Anal. At. Spectrom.* 20
544 (2005) 410–416. doi:10.1039/B415717F.
- 545 [17] L.I.L. Balcaen, B. De Samber, K. De Wolf, F. Cuyckens, F. Vanhaecke, Hyphenation of
546 reverse-phase HPLC and ICP-MS for metabolite profiling—application to a novel
547 antituberculosis compound as a case study, *Anal. Bioanal. Chem.* 389 (2007) 777–786.
548 doi:10.1007/s00216-007-1303-2.
- 549 [18] K.D. Wolf, L. Balcaen, E.V.D. Walle, F. Cuyckens, F. Vanhaecke, A comparison between
550 HPLC-dynamic reaction cell-ICP-MS and HPLC-sector field-ICP-MS for the detection of
551 glutathione-trapped reactive drug metabolites using clozapine as a model compound, *J.*
552 *Anal. At. Spectrom.* 25 (2010) 419–425. doi:10.1039/B921638C.
- 553 [19] K.L. Ackley, K.L. Sutton, J.A. Caruso, A comparison of nebulizers for microbore LC-ICP-
554 MS with mobile phases containing methanol, *J. Anal. At. Spectrom.* 15 (2000) 1069–
555 1073. doi:10.1039/B000986P.

- 556 [20] S. Döker, İ.İ. Boşgelmez, Rapid extraction and reverse phase-liquid chromatographic
557 separation of mercury(II) and methylmercury in fish samples with inductively coupled
558 plasma mass spectrometric detection applying oxygen addition into plasma, *Food*
559 *Chem.* 184 (2015) 147–153. doi:10.1016/j.foodchem.2015.03.067.
- 560 [21] S. Trümpler, S. Nowak, B. Meermann, G.A. Wiesmüller, W. Buscher, M. Sperling, U.
561 Karst, Detoxification of mercury species—an in vitro study with antidotes in human
562 whole blood, *Anal. Bioanal. Chem.* 395 (2009) 1929–1935.
- 563 [22] F. Moreno, T. García-Barrera, J.L. Gómez-Ariza, Simultaneous speciation and
564 preconcentration of ultra trace concentrations of mercury and selenium species in
565 environmental and biological samples by hollow fiber liquid phase microextraction
566 prior to high performance liquid chromatography coupled to inductively coupled
567 plasma mass spectrometry, *J. Chromatogr. A.* 1300 (2013) 43–50.
568 doi:10.1016/j.chroma.2013.02.083.
- 569 [23] B. Klencsár, E. Bolea-Fernandez, M.R. Flórez, L. Balcaen, F. Cuyckens, F. Lynen, F.
570 Vanhaecke, Determination of the total drug-related chlorine and bromine contents in
571 human blood plasma using high performance liquid chromatography–tandem ICP-mass
572 spectrometry (HPLC–ICP-MS/MS), *J. Pharm. Biomed. Anal.* 124 (2016) 112–119.
573 doi:10.1016/j.jpba.2016.02.019.
- 574 [24] B. Meermann, A. Hulstaert, A. Laenen, C. Van Looveren, M. Vliegen, F. Cuyckens, F.
575 Vanhaecke, HPLC/ICP-MS in Combination with “Reverse” Online isotope dilution in
576 drug metabolism studies, *Anal. Chem.* 84 (2012) 2395–2401.
577 doi:dx.doi.org/10.1021/ac203165p.
- 578 [25] B.P. Jensen, C.J. Smith, C. Bailey, C. Rodgers, I.D. Wilson, J.K. Nicholson, Application of
579 inductively coupled plasma mass spectrometry and high-performance liquid
580 chromatography-with parallel electrospray mass spectrometry to the investigation of
581 the disposition and metabolic fate of 2-, 3- and 4-iodobenzoic acids in the rat, *J.*
582 *Chromatogr. B Analyt. Technol. Biomed. Life. Sci.* 809 (2004) 279–285.
583 doi:10.1016/j.jchromb.2004.06.038.
- 584 [26] H. Chen, J. Chen, W. Jin, D. Wei, Determination of trace mercury species by high
585 performance liquid chromatography–inductively coupled plasma mass spectrometry
586 after cloud point extraction, *Volume* 172 (2009) 1282–1287.
587 doi:http://dx.doi.org/10.1016/j.jhazmat.2009.07.134.

- 588 [27] C. Gabel-Jensen, K. Lunøe, K.G. Madsen, J. Bendix, C. Cornett, S. Stürup, H.R. Hansen, B.
589 Gammelgaard, Separation and identification of the selenium-sulfur amino acid S-
590 (methylseleno)cysteine in intestinal epithelial cell homogenates by LC-ICP-MS and LC-
591 ESI-MS after incubation with methylseleninic acid, *J. Anal. At. Spectrom.* 23 (2008) 727–
592 732. doi:10.1039/B715899H.
- 593 [28] C. Gabel-Jensen, J. Odgaard, C. Skonberg, L. Badolo, B. Gammelgaard, LC-ICP-MS and
594 LC-ESI-(MS)_n identification of Se-methylselenocysteine and selenomethionine as
595 metabolites of methylseleninic acid in rat hepatocytes, *J. Anal. At. Spectrom.* 24 (2008)
596 69–75. doi:10.1039/B807805J.
- 597 [29] D. Xie, J. Mattusch, R. Wennrich, Separation of Organoarsenicals by Means of
598 Zwitterionic Hydrophilic Interaction Chromatography (ZIC[®]-HILIC) and Parallel ICP-
599 MS/ESI-MS Detection, *Eng. Life Sci.* 8 (2008) 582–588. doi:10.1002/elsc.200800041.
- 600 [30] J. Far, H. Preud'homme, R. Lobinski, Detection and identification of hydrophilic
601 selenium compounds in selenium-rich yeast by size exclusion-microbore normal-phase
602 HPLC with the on-line ICP-MS and electrospray Q-TOF-MS detection, *Anal. Chim. Acta.*
603 657 (2010) 175–190. doi:10.1016/j.aca.2009.10.040.
- 604 [31] T. Falta, G. Koellensperger, A. Standler, W. Buchberger, R.M. Mader, S. Hann,
605 Quantification of cisplatin, carboplatin and oxaliplatin in spiked human plasma samples
606 by ICP-SFMS and hydrophilic interaction liquid chromatography (HILIC) combined with
607 ICP-MS detection, *J. Anal. At. Spectrom.* 24 (2009) 1336–1342. doi:10.1039/B907011G.
- 608 [32] T. Grevenstuk, P. Flis, L. Ouerdane, R. Lobinski, A. Romano, Identification of the tri-Al
609 tricitrate complex in *Plantago almogravensis* by hydrophilic interaction LC with parallel
610 ICP-MS and electrospray Orbitrap MS/MS detection, *Metallomics.* 5 (2013) 1285–1293.
611 doi:10.1039/C3MT00101F.
- 612 [33] R. Rellán-Álvarez, J. Giner-Martínez-Sierra, J. Orduna, I. Orera, J.Á. Rodríguez-Castrillón,
613 J.I. García-Alonso, J. Abadía, A. Álvarez-Fernández, Identification of a Tri-Iron(III), Tri-
614 Citrate Complex in the Xylem Sap of Iron-Deficient Tomato Resupplied with Iron: New
615 Insights into Plant Iron Long-Distance Transport, *Plant Cell Physiol.* 51 (2010) 91–102.
616 doi:10.1093/pcp/pcp170.
- 617 [34] J. Vidmar, A. Martinčič, R. Milačič, J. Ščančar, Speciation of cisplatin in environmental
618 water samples by hydrophilic interaction liquid chromatography coupled to inductively

- 619 coupled plasma mass spectrometry, *Talanta*. 138 (2015) 1–7.
620 doi:10.1016/j.talanta.2015.02.008.
- 621 [35] A. Leclercq, A. Nonell, J.L. Todolí Torró, C. Bresson, L. Vio, T. Vercoouter, F. Chartier,
622 Tutorial: Introduction of organic/hydro-organic matrices in inductively coupled plasma
623 optical emission spectrometry and mass spectrometry: A tutorial review. Part I.
624 Theoretical considerations, *Anal. Chim. Acta.* 885 (2015) 33–56.
625 doi:10.1016/j.aca.2015.03.049.
- 626 [36] A. Leclercq, A. Nonell, J.L. Todolí Torró, C. Bresson, L. Vio, T. Vercoouter, F. Chartier,
627 Tutorial: Introduction of organic/hydro-organic matrices in inductively coupled plasma
628 optical emission spectrometry and mass spectrometry: A tutorial review. Part II.
629 Practical considerations, *Anal. Chim. Acta.* 885 (2015) 57–91.
630 doi:10.1016/j.aca.2015.04.039.
- 631 [37] B. Klencsár, L. Balcaen, F. Cuyckens, F. Lynen, F. Vanhaecke, Development and
632 validation of a novel quantification approach for gradient elution reversed phase high-
633 performance liquid chromatography coupled to tandem ICP-mass spectrometry (RP-
634 HPLC-ICP-MS/MS) and its application to diclofenac and its related compounds, *Anal.*
635 *Chim. Acta.* 974 (2017) 43–53. doi:10.1016/j.aca.2017.04.030.
- 636 [38] M. Martin, C. Eon, G. Guiochon, Study of the pertinency of pressure in liquid
637 chromatography, *J. Chromatogr. A.* 108 (1975) 229–241. doi:10.1016/S0021-
638 9673(00)84666-X.
- 639 [39] J.J. van Deemter, F.J. Zuiderweg, A. Klinkenberg, Longitudinal diffusion and resistance
640 to mass transfer as causes of nonideality in chromatography, *Chem. Eng. Sci.* 5 (1956)
641 271–289. doi:10.1016/0009-2509(56)80003-1.
- 642 [40] J.H. Knox, M. Saleem, Kinetic Conditions for Optimum Speed and Resolution in Column
643 Chromatography, *J. Chromatogr. Sci.* 7 (1969) 614–622.
644 doi:10.1093/chromsci/7.10.614.
- 645 [41] L.R. Snyder, J.W. Dolan, J.R. Gant, Gradient elution in high-performance liquid
646 chromatography : I. Theoretical basis for reversed-phase systems, *J. Chromatogr. A.* 165
647 (1979) 3–30. doi:10.1016/S0021-9673(00)85726-X.
- 648 [42] A. D’Attoma, C. Grivel, S. Heinisch, On-line comprehensive two-dimensional separations
649 of charged compounds using reversed-phase high performance liquid chromatography
650 and hydrophilic interaction chromatography. Part I: Orthogonality and practical peak

651 capacity considerations, *J. Chromatogr. A.* 1262 (2012) 148–159.
652 doi:10.1016/j.chroma.2012.09.028.

653 [43] M. Wind, A. Eisenmenger, W. D. Lehmann, Modified direct injection high efficiency
654 nebulizer with minimized dead volume for the analysis of biological samples by micro-
655 and nano-LC-ICP-MS, *J. Anal. At. Spectrom.* 17 (2002) 21–26. doi:10.1039/B108153P.

656 [44] Z. Stefánka, G. Koellensperger, G. Stingeder, S. Hann, Down-scaling narrowbore LC-ICP-
657 MS to capillary LC-ICP-MS: a comparative study of different introduction systems, *J.*
658 *Anal. At. Spectrom.* 21 (2006) 86–89. doi:10.1039/B511629E.

659 [45] G. Zoorob, M. Tomlinson, J. Wang, J. Caruso, Evaluation of the direct injection nebulizer
660 in the coupling of high-performance liquid chromatography to inductively coupled
661 plasma mass spectrometry, *J. Anal. At. Spectrom.* 10 (1995) 853–858.
662 doi:10.1039/JA9951000853.

663 [46] P. Giusti, D. Schaumlöffel, J.R. Encinar, J. Szpunar, Interfacing reversed-phase nanoHPLC
664 with ICP-MS and on-line isotope dilution analysis for the accurate quantification of
665 selenium-containing peptides in protein tryptic digests, *J. Anal. At. Spectrom.* 20 (2005)
666 1101–1107. doi:10.1039/B506620D.

667 [47] S.S. Kannamkumarath, R.G. Wuilloud, A. Stalcup, J.A. Caruso, H. Patel, A. Sakr,
668 Determination of levothyroxine and its degradation products in pharmaceutical tablets
669 by HPLC-UV-ICP-MS, *J. Anal. At. Spectrom.* 19 (2004) 107–113. doi:10.1039/B307970H.

670 [48] L. Rottmann, K.G. Heumann, Development of an on-line isotope dilution technique with
671 HPLC/ICP-MS for the accurate determination of elemental species, *Fresenius J. Anal.*
672 *Chem.* 350 (1994) 221–227. doi:10.1007/BF00322473.

673 [49] G. Raber, R. Raml, W. Goessler, K.A. Francesconi, Quantitative speciation of arsenic
674 compounds when using organic solvent gradients in HPLC-ICPMS, *J. Anal. At. Spectrom.*
675 25 (2010) 570–576. doi:10.1039/B921881E.

676 [50] J.-L. Todoli, J.-M. Mermet, *Liquid Sample Introduction in ICP Spectrometry : A Practical*
677 *Guide*, Elsevier Science, Amsterdam, 2008.

678 [51] B.W. Acon, J.A. McLean, A. Montaser, A direct injection high efficiency nebulizer
679 interface for microbore high-performance liquid chromatography-inductively coupled
680 plasma mass spectrometry, *J. Anal. At. Spectrom.* 16 (2001) 852–857.
681 doi:10.1039/B103085J.

- 682 [52] J.L. Todoli, M. Grotti, Fast determination of arsenosugars in algal extracts by narrow
683 bore high-performance liquid chromatography-inductively coupled plasma mass
684 spectrometry, *J Chromatogr.* 1217 (n.d.) 7428–7433.
- 685 [53] K.E. Lokits, P.A. Limbach, J.A. Caruso, Interfaces for capillary LC with ICPMS detection: A
686 comparison of nebulizers/spray chamber configurations, *J. Anal. At. Spectrom.* 24
687 (2009) 528–534. doi:10.1039/B820121H.
- 688 [54] Juan Manuel Marchante-Gayo, Christoph Thomas, Ingo Feldmann, Norbert Jakubowski,
689 Comparison of different nebulisers and chromatographic techniques for the speciation
690 of selenium in nutritional commercial supplements by hexapole collision an react cell
691 ICP-MS, *J Anal Spectrom.* 15 (2000) 1093–1102. doi:DOI: 10.1039/b002372h.
- 692 [55] L.H. Møller, A. Macherius, T.H. Hansen, H.M. Nielsen, C. Cornett, J. Østergaard, S.
693 Stürup, B. Gammelgaard, Quantification of pharmaceutical peptides in human plasma
694 by LC-ICP-MS sulfur detection, *J. Anal. At. Spectrom.* 31 (2016) 1877–1884.
695 doi:10.1039/C6JA00132G.
- 696 [56] B.-O. Axelsson, M. Jörnten-Karlsson, P. Michelsen, F. Abou-Shakra, The potential of
697 inductively coupled plasma mass spectrometry detection for high-performance liquid
698 chromatography combined with accurate mass measurement of organic
699 pharmaceutical compounds, *Rapid Commun. Mass Spectrom.* 15 (2001) 375–385.
700 doi:10.1002/rcm.238.
- 701 [57] B.P. Jensen, B. Gammelgaard, S.H. Hansen, J.V. Andersen, Comparison of direct
702 injection nebulizer and desolvating microconcentric nebulizer for analysis of chlorine-,
703 bromine- and iodine-containing compounds by reversed phase HPLC with ICP-MS
704 detection, *J. Anal. At. Spectrom.* 18 (2003) 891–896. doi:10.1039/B304651F.
- 705 [58] J. Chen, H. Chen, X. Jin, H. Chen, Determination of ultra-trace amount methyl-, phenyl-
706 and inorganic mercury in environmental and biological samples by liquid
707 chromatography with inductively coupled plasma mass spectrometry after cloud point
708 extraction preconcentration, *Talanta.* 77 (2009) 1381–1387.
709 doi:10.1016/j.talanta.2008.09.021.
- 710 [59] D.S. Vidler, R.O. Jenkins, J.F. Hall, C.F. Harrington, The determination of methylmercury
711 in biological samples by HPLC coupled to ICP-MS detection, *Appl. Organomet. Chem.* 21
712 (2007) 303–310. doi:10.1002/aoc.1173.

- 713 [60] M. Birka, C.A. Wehe, L. Telgmann, M. Sperling, U. Karst, Sensitive quantification of
714 gadolinium-based magnetic resonance imaging contrast agents in surface waters using
715 hydrophilic interaction liquid chromatography and inductively coupled plasma sector
716 field mass spectrometry, *J. Chromatogr. A.* 1308 (2013) 125–131.
717 doi:10.1016/j.chroma.2013.08.017.
- 718 [61] L. Telgmann, C.A. Wehe, J. Künnemeyer, A.-C. Bülter, M. Sperling, U. Karst, Speciation
719 of Gd-based MRI contrast agents and potential products of transmetalation with iron
720 ions or parenteral iron supplements, *Anal. Bioanal. Chem.* 404 (2012) 2133–2141.
721 doi:10.1007/s00216-012-6404-x.
- 722 [62] P. Hemström, Y. Nygren, E. Björn, K. Irgum, Alternative organic solvents for HILIC
723 separation of cisplatin species with on-line ICP-MS detection, *J. Sep. Sci.* 31 (2008) 599–
724 603. doi:10.1002/jssc.200700480.
- 725 [63] S. Trümpler, W. Lohmann, B. Meermann, W. Buscher, M. Sperling, U. Karst, Interaction
726 of thimerosal with proteins—ethylmercury adduct formation of human serum albumin
727 and β -lactoglobulin A, *Metallomics.* 1 (2009) 87–91. doi:10.1039/B815978E.
- 728 [64] J. Hogeback, M. Schwarzer, C.A. Wehe, M. Sperling, U. Karst, Investigating the adduct
729 formation of organic mercury species with carbonic anhydrase and hemoglobin from
730 human red blood cell hemolysate by means of LC/ESI-TOF-MS and LC/ICP-MS,
731 *Metallomics.* 8 (2016) 101–107. doi:10.1039/C5MT00186B.
- 732 [65] S.C. Shum, R. Neddersen, R.S. Houk, Elemental speciation by liquid chromatography-
733 inductively coupled plasma mass spectrometry with direct injection nebulization, *The*
734 *Analyst.* 117 (1992) 577–582.
- 735 [66] G. Caumette, C.-P. Lienemann, I. Merdrignac, H. Paucot, B. Bouyssiére, R. Lobinski,
736 Sensitivity improvement in ICP MS analysis of fuels and light petroleum matrices using a
737 microflow nebulizer and heated spray chamber sample introduction, *Talanta.* 80 (2009)
738 1039–1043. doi:10.1016/j.talanta.2009.08.017.
- 739 [67] M. Wind, A. Eisenmenger, W.D. (analytic) Lehmann, Modified direct injection high
740 efficiency nebulizer with minimized dead volume for the analysis of biological samples
741 by micro- and nano-LC-ICP-MS, *J Anal Spectrom Print.* 17 (2002) 21–26.
- 742 [68] R.G. Brennan, S.-A.E.O. Murdock, M. Farmand, K. Kahen, S. Samii, J.M. Gray, A.
743 Montaser, Nano-HPLC-inductively coupled plasma mass spectrometry for arsenic
744 speciation, *J. Anal. At. Spectrom.* 22 (2007) 1199–1205. doi:10.1039/B703257A.

- 745 [69] L. Bendahl, B. Gammelgaard, O. Jøns, O. Farver, S.H. Hansen, Interfacing capillary
746 electrophoresis with inductively coupled plasma mass spectrometry by direct injection
747 nebulization for selenium speciation, *J. Anal. At. Spectrom.* 16 (2003) 38–42.
748 doi:10.1039/B007137O.
- 749 [70] A. D’Attoma, Développement de méthodes bidimensionnelles en ligne LCxLC-MS pour
750 l’analyse de composés chargés, Lyon 1, 2013. <http://www.theses.fr/2013LYO10214>
751 (accessed April 28, 2016).
- 752 [71] Kurt Hofmann, István Halasz, Mass transfer in ideal and geometrically deformed open
753 tubes. I. Ideal and coiled tubes with circular cross section, *J. Chromatogr. A.* 173 (1979)
754 211–228. doi:doi.org/10.1016/S0021-9673(00)92292-1.

755
756

757 **Figure captions**

758

759 Figure 1: Percentage of remaining plates (β^2) as a function of extra-column variance for
760 different column geometries providing (a) 10000 and (b) 30000 plates. Calculations from
761 Eqs. (6) and (7) with $k_e=3$; $h=3$ and $\epsilon_t=0.7$.

762

763 Figure 2: Relative distribution of nebulizers and spray chambers depending on the column
764 inner diameter. Based on 55 reported studies dealing with LC-ICP-MS for organic matrices
765 (from 1995 to 2017)

766

767 Figure 3: Schematic representation of the instrument set-up for peak variance
768 measurement. F_1 is the total flow-rate delivered by the pump, F_2 is the flow-rate towards UV
769 Detector 2, and F_3 is the flow-rate sent to the waste. Tubing geometry is given in Table 3.

770

771 Figure 4: Variation of the variance due to the tube 1 ($\sigma^2_{\text{Tube 1}}$) as a function of F_1 . See Table 3
772 for tubing geometry and Fig. 3 for instrument set-up. Solute: methylparaben (75 ppm in
773 50/50 Water/MeOH v/v). 1 μL injected. No column. Mobile phase: 50/50 water/MeOH v/v.
774 254 nm.

775

776 Figure 5: Variation of the variance due to the split (σ^2_{split}) with F_2 . (a) effect of the tube i.d.

777 (25 μm and 65 μm) considering the same split ratio (1:4.8). (b) effect of the split ratio (1:4.8,
778 1:9.4 and 1:50. Same other conditions as in Fig.4.

779

780 Figure 6 : Overlay of the peaks obtained in Detector 2 with settings A, B, C, D and E. (a) Same
781 F_1 (100 $\mu\text{L}/\text{min}$) resulting in different F_2 (100, 20.8, 20.8, 10.6, 2 $\mu\text{L}/\text{min}$ respectively) and (b)
782 different F_1 (10, 50, 50, 100, 400 $\mu\text{L}/\text{min}$ respectively) resulting in same F_2 (10 $\mu\text{L}/\text{min}$).
783 Measured extra-column variance (σ^2_{ext}) is indicated at peak apex. Same other conditions as
784 in Fig.4.

Table 1. Optimum flow-rates (F_{opt}), column plate number (N_{col}), column variance (σ^2_{col}) depending on column internal diameter (d_i) and particle diameter (d_p). Calculations performed with $k_e = 3$; $D_m = 10^{-9}$ m²/s; $L = 150$ mm; $v = 5$; $h = 3$; $\epsilon_t = 0.7$, using Eqs. (5) to

	d_i (mm)	$d_p = 5 \mu\text{m}$		$d_p = 1.7 \mu\text{m}$	
		$N_{col} = 10000$		$N_{col} = 30000$	
		F_{opt} ($\mu\text{L}/\text{min}$)	σ^2_{col} (μL^2)	F_{opt} ($\mu\text{L}/\text{min}$)	σ^2_{col} (μL^2)
Conventional	4.6	698	4867	2052	1655
Narrow bore	2.1	145	211	428	72
Micro bore	1	33	11	97	4
Capillary	0.3	3	0.088	9	0.03
Nano bore	0.075	0.2	0.00034	0.5	0.00012

(12).

Table 2. Reported LC-ICP-MS studies on organic matrices. Evaluation of the percentage of remaining plates (β^2). Calculations with a retention factor of 3, from Eqs. (1) to (12), with S = 4 (small molecules) and S = 50 (large molecules).

[Ref] (Figure)	Sample	LC conditions (Elution mode, column dimension, gradient)	Nebulizer		Spray chamber			β^2 (%)
			Type	Brand	Type	Brand	Cooling	
Conventional column								
[17] (Fig. 3)	Standards, urine, faeces from dog and rat, ¹⁴ C	RPLC, C18, (250 x 4.6 mm, 5 μ m), 1000 μ L/min Gradient (Phase A: 0.1 M ammonium acetate pH 7.5, Phase B: 10 % 1 M ammonium acetate pH 7.5–45 % MeOH–45 % ACN)	Micro-concentric	PFA-LC	Cyclonic	PC ³	2°C	24
([24], Fig 2)	Antituberculosis drug, ⁸¹ Br	RPLC, C18 (250 x 4.6 mm, 5 μ m), 1000 μ L/min Gradient (Phase A: 0.1 mol/L ammonium acetate buffer, Phase B: 10 % 1 mol/L ammonium acetate, 45 % MeOH, 45 % ACN)	Micro-concentric	ES-2050 microflow PFA-LC	Cyclonic	PC ³	2°C	16
[20], Fig 1	Standards Fish, Hg	RPLC, C18 (100 x 4.6 mm, 3.5 μ m), 450 μ L/min Isocratic (55 % MeOH + 0.1 % mercaptoethanol + 45 % 60 mM ammonium acetate, pH 4.0)	Micro-concentric	MicroMist	nd	nd	nd	31
([25], Fig 1)*	Urine and bile in rat, ¹²⁷ I	RPLC, C18 (150 x 4.6 mm, 3 μ m), 1000 μ L/min Isocratic (30 % ACN + 0.1 % formic acid for analysis of 3- and 4-iodobenzoic acid metabolites or 20 % ACN + 0.1 % formic acid for analysis of 2-iodobenzoic acid metabolites)	Micro-concentric	PFA concentric	Double pass	nd	-7°C	14
([58], Fig 2)	Human hair, fish sample, Hg	RPLC, C18 (150 x 4.6 mm, 5 μ m), 800 μ L/min Isocratic (35 % MeOH + 40 % ACN + 25 % water containing 1.0x10 ⁻⁴ mol/L)	nd	nd	nd	nd	nd	34
([26], Fig 1)	Standards, Hg	RPLC, C18 (150 x 4.6 mm, 5 μ m), 700 μ L/min Isocratic (90 % (v/v) MeOH–10 % (v/v) water containing DDTc 1.0x10 ⁻⁴ mol/L)	nd	nd	nd	nd	-5°C	86
Narrow bore column								
([59], Fig 1)	Standard Fish tissue and hair, Hg,	RPLC, C18 (150 x 3.2 mm, 3 μ m), 400 μ L/min Isocratic (50 % MeOH + 50 % water (v/v) with 0.01 % 2-mercaptoethanol)	Micro-concentric	Microflow PFA	nd	nd	-5°C	59
([60], Fig 3)	Standards from pharmaceutical companies, Gd,	HILIC, (150 x 2.1 mm, 3 μ m), 250 μ L/min Isocratic (Phase A: 50 mmol/L aqueous ammonium formate, Phase B: ACN, 30 % A and 70 % B)	Micro-concentric	PFA microflow ST	Cyclonic	nd	-7°C	<5
([60], Fig 4)					Desolvation unit	APEX Q	-5°C	<5
(66), Fig 2)	Blood plasma, Fe,	HILIC, (150 x 2.1 mm, 3 μ m), 250 μ L/min Isocratic (Phase A: 25 mmol/L aqueous ammonium acetate, Phase B: ACN, 30 % A and 70 % B)	Micro-concentric	PFA microflow ST	Cyclonic	nd	-5°C	18
([33], Fig 1)	Standards Xylem sample, ⁵⁴ Fe	HILIC, (150 x 2.1 mm, 5 μ m), 100 μ L/min Gradient (Phase A: 10 mM ammonium acetate in water Phase B: 10 mM ammonium acetate in MeOH)	nd	nd	nd	nd	nd	14
([63], Fig 2)	Human serum, ²⁰² Hg	RPLC, C5 (150 x 2.1 mm, 5 μ m), 300 μ L/min Gradient (Phase A: 0.1 % formic acid in water, Phase B: ACN)	Concentric	Meinhard nebulizer TR-30-A3	nd	PC3	nd	8
([64], Fig 4)	Carbonic anhydrase, thimerosal, ²⁰² Hg	RPLC, C18 (150 x 2.1 mm, 5 μ m), 300 μ L/min Gradient (Phase A: 0.1 % acid formic in water, Phase B: ACN)	Micro-concentric	PFA MicroFlow	Cyclonic	nd	-5°C	8
([9], Fig 1)	Standards Human cell, Pt	HILIC, (150 x 2.1 mm, 5 μ m), 100 μ L/min Isocratic (70 % DMF + 30 % 20 mM ammonium acetate or 70 % ACN + 30 % 20 mM ammonium acetate)	Parallel path	MiraMist	Cyclonic	nd	5°C	11

[Ref] (Figure)	Sample	LC conditions (Elution mode, column dimension, gradient)	Nebulizer		Spray chamber			β^2 (%)
			Type	Brand	Type	Brand	Cooling	
[[52], Fig 2)	Standards Arsenosugars in algal extract, As	Anion Exchange, (100 x 2.1 mm, 5 μ m), 100 μ L/min Isocratic (60 mM aqueous ammonium dihydrogen phosphate of pH 5.9)	Micro-concentric	PFA-ST (Dead volume 13 μ L)	Cyclonic	Cinnabar (20 mL)	nd	70
[[29], Fig 1)	Standards, ⁷⁵ As	HILIC, (50 x 2.1 mm, 3.5 μ m), 100 μ L/min Isocratic (70 % ACN + 20 % 125 mM ammonium acetate pH 8.3)	Micro-concentric	Micro-concentric	Scott double pass	nd	nd	<5
[[19], Fig 4)	Standards, Sn	RPLC, C18 (150 x 2 mm, 5 μ m), 200 μ L/min Isocratic (70 % (v/v) MeOH + 29 % (v/v) water + 1 % (v/v) glacial acetic acid and 4 mM ion pair reagent (1-pentansulfonic acid sodium salt 1-hydrate))	Nd	nd	nd	nd	nd	17
[[28], Fig 1)	Rat hepatocyte, ⁸² Se	RPLC, C18 (250 x 2 mm, 5 μ m), 200 μ L/min Gradient (Phase A: 0.1 % formic acid 2% MeOH, Phase B: 0.1 % formic acid in 50 % MeOH)	Micro-concentric	MicroMist	Cyclonic	PC3	4°C	50
[[47], Fig 5)*	Standards, ¹²⁷ I	RPLC, (250 x 2 mm, 5 μ m), 300 μ L/min Isocratic (22 % (v/v) ACN ; 0.08 % (v/v) trifluoroacetic acid), Before going to the ICP-MS using make-up solution 2 % (v/v) HNO ₃ ; (0.7 ml/min)	Cross-flow	Gem Tip (Perkin Elmer)	Double pass	Ryto	nd	6
Microbore column								
[[31], Fig 3)	Plasma Sample Cisplatin, ¹⁹⁵ Pt	HILIC, (150 x 1 mm, 3 μ m), 90 μ L/min Gradient (Phase A: 95 % ACN, 5 % water, 0.05 % formic acid, Phase B: 5 % ACN, 95 % water, 0.05 % formic acid)	Micro-concentric	PFA-ST nebulizer	Cyclonic	PC3	-5°C	<5
[[70], Fig 5)	Fish liver and muscle, Hg, Pb	RPLC, C18 (150 x 1 mm, 5 μ m), 120 μ L/min Isocratic (0.2 % (v/v) 2-mercaptoethanol, 174.2 mg/L SPS, 12 % (v/v) MeOH and 1 mg/L EDTA, pH 2.8)	Total consumption nebulizer DIHEN-170-AA					<5
[[71], Fig 1)	Arsenic species Urine, As	Anion Exchange, (150 x 1 mm, 5 μ m), 100 μ L/min Isocratic (20 mM mono-ammonium dihydrogen phosphate acid and diammonium hydrogen phosphate buffer)	Total consumption nebulizer DIN (Microneb 2000)					<5
[[71], Fig 1)	Arsenic species Urine, As	Anion exchange, (150 x 1 mm, 5 μ m), 100 μ L/min Isocratic (20 mM mono-ammonium dihydrogen phosphate acid and diammonium hydrogen phosphate buffer)	Micro-concentric	Micro-concentric nebulizer (MCN-100)	Double pass	Scott Ryton	nd	<5
[[71], Fig 1)	Arsenic species Urine, As	Anion exchange, 5 (150 x 1 mm, 5 μ m), 100 μ L/min Isocratic (20 mM mono-ammonium dihydrogen phosphate acid and diammonium hydrogen phosphate buffer)	Cross flow	nd	Double pass	Scott Ryton	nd	<5
[[55], Fig 3)	Standards, Hg	RPLC, C18 (50 x 1 mm, 3.5 μ m), 100 μ L/min Isocratic (Cobalamin: 25 mM ammonium acetate, 10 % ACN, Organomercury and lead: 7.5 mM PIC-B5, 20 % ACN)	Total consumption nebulizer DIHEN (reduce by inserting a 0.008 in id tubing into the nebulizer)					<5
	Standards, Pb							
	Standards, Co							
Capillary column								
[[67], Fig 5)*	Standards Synthetic phosphopeptide,	RPLC, C18 (250 x 0.3 mm, 5 μ m), 116 μ L/min Gradient (Phase A: 100/0.065 water/TFA, Phase B: 80/20/0.05 ACN/water/TFA)	Total consumption nebulizer Modified DIHEN					<1
[[67], Fig 5)*	²³⁸ U, ¹¹⁵ In, ¹²⁷ I, ³¹ P	RPLC, C18 (250 x 0.3 mm, 5 μ m), 116 μ L/min Gradient (Phase A: 100/0.065 water/TFA, Phase B: 80/20/0.05 ACN/water/TFA)	Micro-concentric	PFA-LC	Cyclonic	PFA	Nd	<1

nd: not determined or not found in the literature

* : use of flow splitting

Table 3. Tubing geometry and split ratio (calculated and measured) for Setting A, B, C, D and E (see Fig. 3 for instrument set-up). Split ratio were calculated from Eq. (13).

	Setting A	Setting B	Setting C	Setting D	Setting E
Tube 1	60 cm x 100 μ m				
Tube 3	-	62 cm x 100 μ m	44.5 cm x 65 μ m	24 cm x 100 μ m	132 cm x 127 μ m
Tube 2	-	29 cm x 65 μ m	6 cm x 25 μ m	56 cm x 65 μ m	9 cm x 25 μ m
Calculated split ratio	1:1	1:3.6	1:7.4	1:14	1:45
Measured split ratio	1:1	1:4.8	1:4.8	1:9.4	1:50

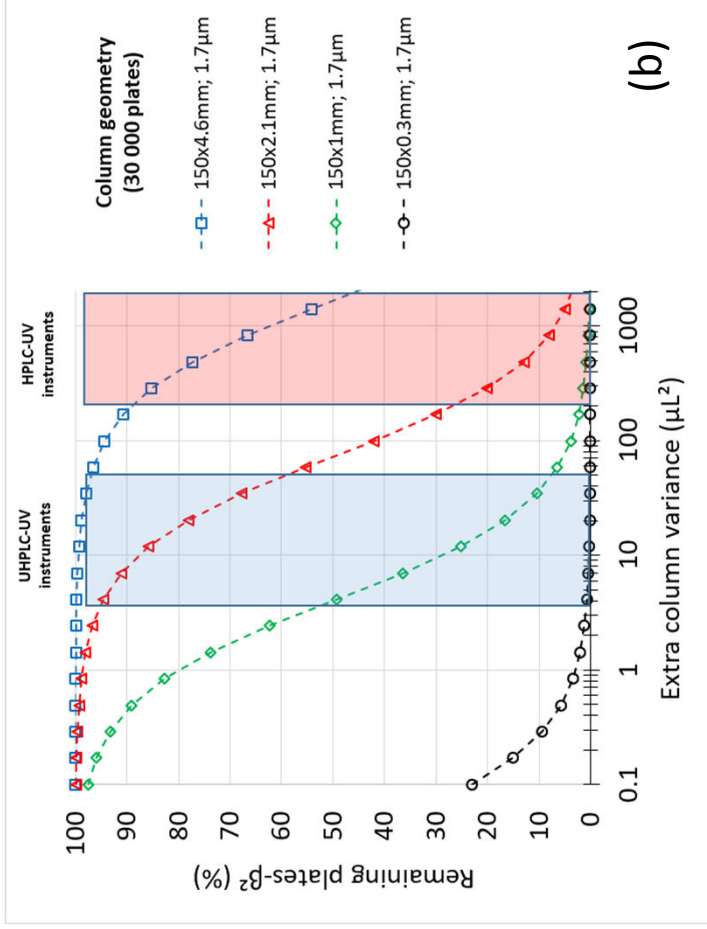
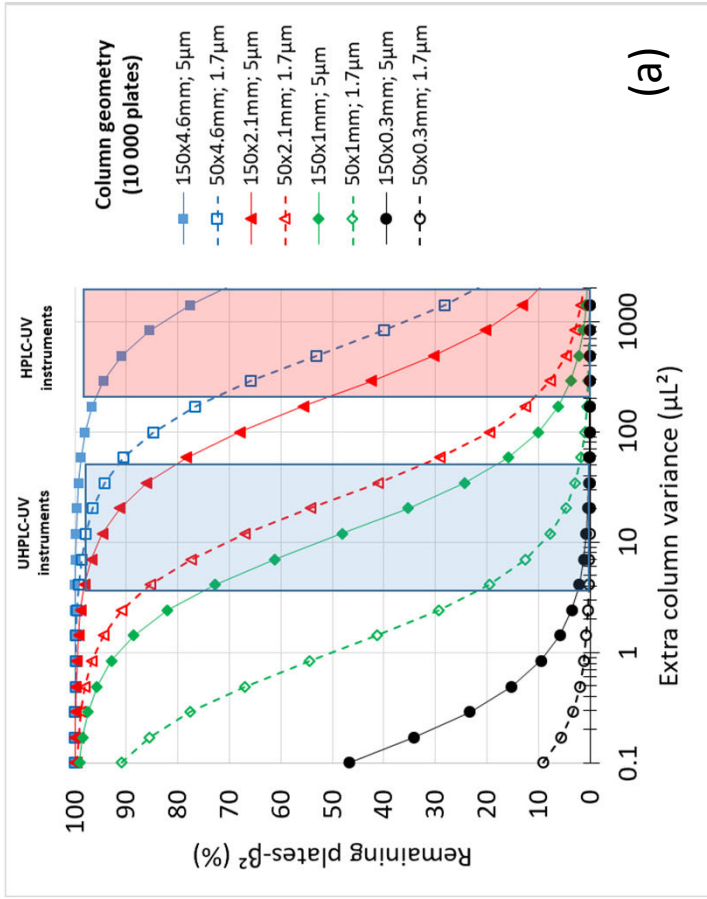


Figure 1

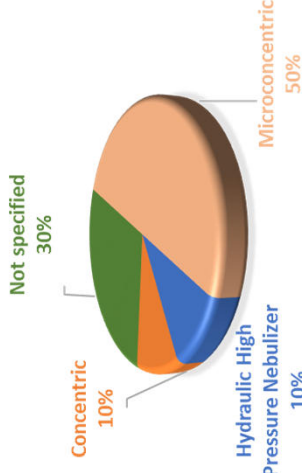
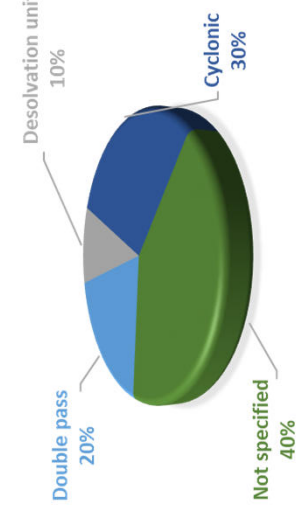
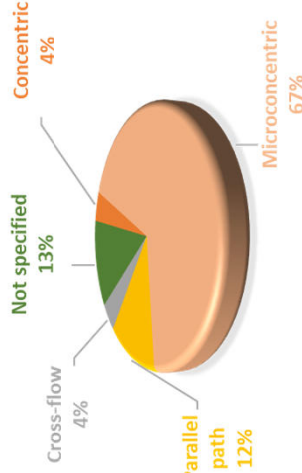
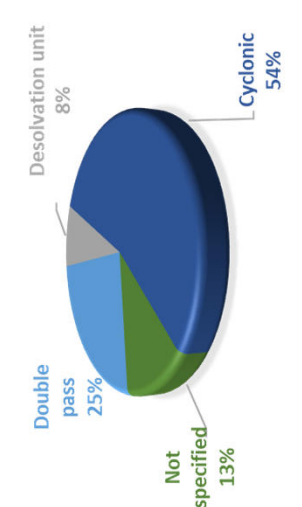
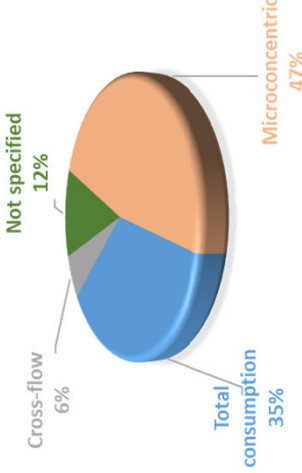
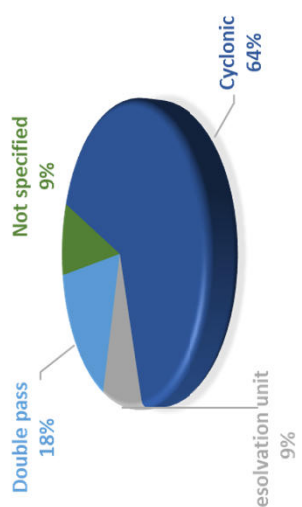
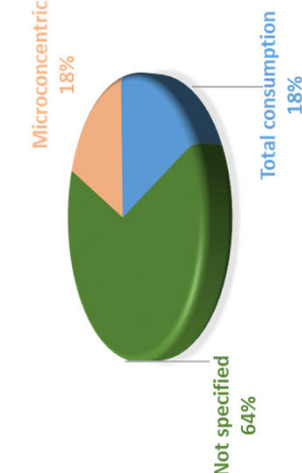
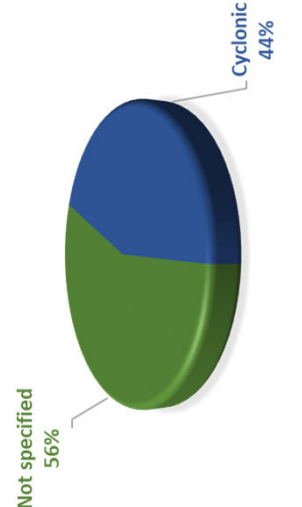
Column	Nebulizer	Spray Chamber
Conventional (10 studies)	 <p>Not specified 30%</p> <p>Concentric 10%</p> <p>Hydraulic High Pressure Nebulizer 10%</p> <p>Microconcentric 50%</p>	 <p>Double pass 20%</p> <p>Desolvation unit 10%</p> <p>Cyclonic 30%</p> <p>Not specified 40%</p>
Narrow bore (24 studies)	 <p>Not specified 13%</p> <p>Concentric 4%</p> <p>Cross-flow 4%</p> <p>Parallel path 12%</p> <p>Microconcentric 67%</p>	 <p>Double pass 25%</p> <p>Desolvation unit 8%</p> <p>Cyclonic 54%</p> <p>Not specified 13%</p>
Microbore bore (17 studies)	 <p>Not specified 12%</p> <p>Cross-flow 6%</p> <p>Total consumption 35%</p> <p>Microconcentric 47%</p>	 <p>Double pass 18%</p> <p>Not specified 9%</p> <p>Desolvation unit 9%</p> <p>Cyclonic 64%</p>
Capillary (11 studies)	 <p>Not specified 64%</p> <p>Microconcentric 18%</p> <p>Total consumption 18%</p>	 <p>Not specified 56%</p> <p>Cyclonic 44%</p>

Figure 2

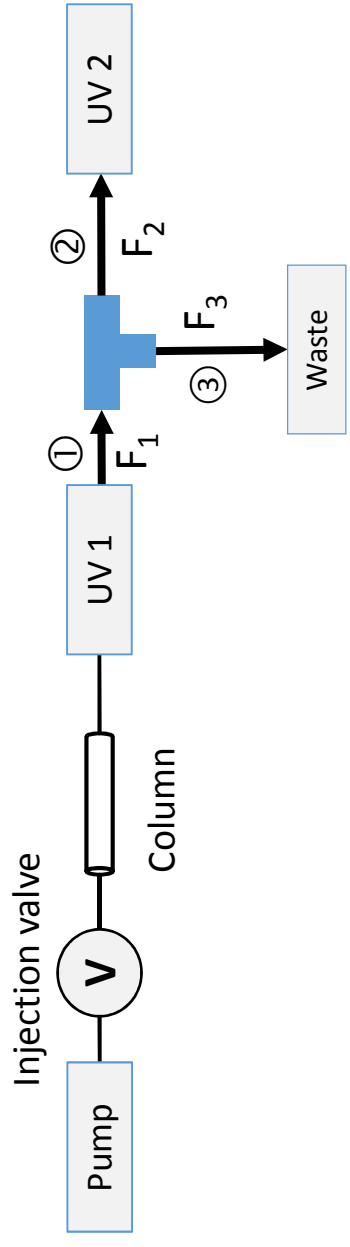


Figure 3

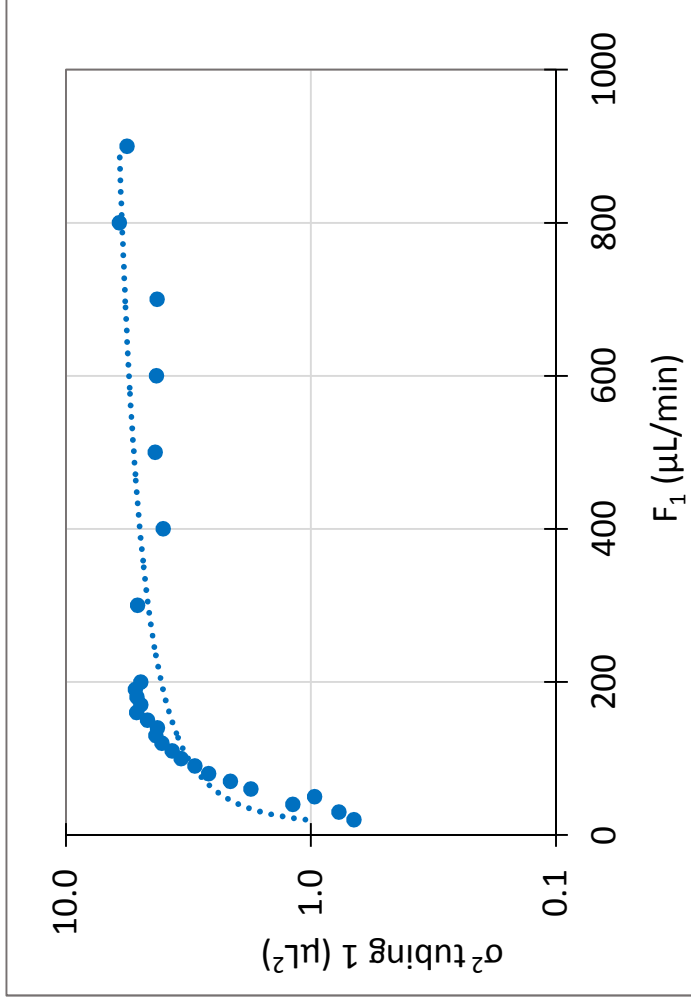


Figure 4

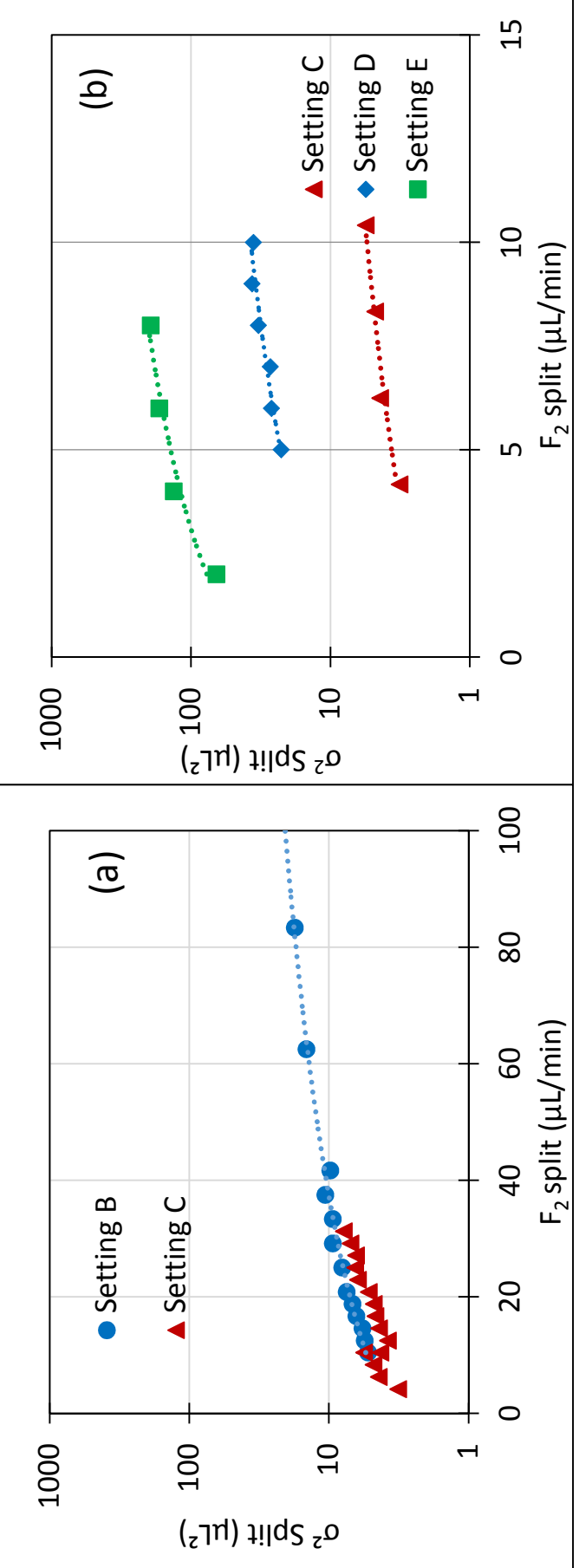


Figure 5

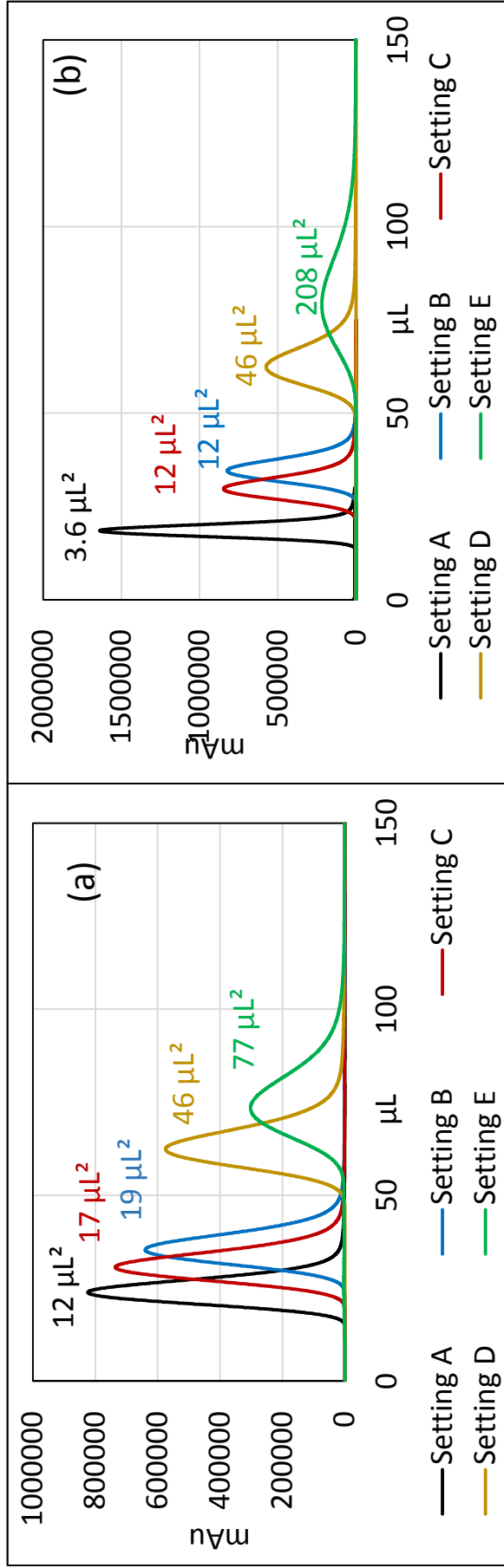


Figure 6